Photoexcitation of the P_4^{480} state induces a secondary photocycle that potentially desensitizes channelrhodopsin-2.

Mattia Saita[†], Franziska Pranga-Sellnau[†], Tom Resler[†], Ramona Schlesinger[‡], Joachim Heberle[†], and Victor A. Lorenz-Fonfria[§,*]

[†]Experimental Molecular Biophysics, Department of Physics, Freie Universität Berlin, 14195 Berlin, Germany; [‡]Genetic Biophysics, Department of Physics, Freie Universität Berlin, 14195 Berlin, Germany; [§]Institute of Molecular Science, Universitat de València, 46980 Paterna, Spain; and Department of Biochemistry and Molecular Biology, Universitat de València, 46100 Burjassot, Spain.

ABSTRACT: Channelrhodopsins (ChRs) are light-gated cation channels. In spite their wide use to activate neurons with light, the photocurrents of ChRs rapidly decay in intensity under both continuous illumination and fast trains of light pulses, broadly referred to as desensitization. This undesirable phenomenon has been explained by two interconnected photocycles, each of them containing a non-conductive dark state (D1 and D2) and a conductive state (O1 and O2). While the D1 and O1 states correspond to the dark-state and P_3^{520} intermediate of the primary all-*trans* photocycle of ChR2, the molecular identity of D2 and O2 remains unclear. We show that P_4^{480}, the last intermediate of the all-*trans* photocycle, is photoactive. Its photocycle, characterized by time-resolved UV/Vis spectroscopy, contains a red-shifted intermediate, I_3^{530}. Our results indicate that the D2 and O2 states correspond to the P_4^{480} and I_3^{530} intermediates, connecting desensitization of ChR2 with the photochemical properties of the P_4^{480} intermediate.

INTRODUCTION

Channelrhodopsins (ChRs) are membrane proteins belonging to the family of microbial rhodopsins, with a covalently linked retinal chromophore.[1] ChR2 from *Chlamydomonas reinhardtii*, *Cr*ChR2, a light-gated cation-conductive channel,[2] is widely used in optogenetics[3] and has been studied in detail by electrophysiology and molecular spectroscopies.[4,5] The non-conductive dark state of *Cr*ChR2, whose structure was recently solved by X-ray crystallography,[6] bears retinal in all-*trans*,15-*anti* configuration,[7,8] hereafter ChR^{470} state. Depending on the illumination history we also find in the dark minor proportions (up to 25-30%) of *Cr*ChR2 with 13-*cis*,15-*syn* retinal,[8,9] hereafter ChR^{460} state. [Superscripts refer to the approximate λ^{max} of the retinal in nm.]

The most detailed spectroscopic investigations on *Cr*ChR2 and related ChRs have used illumination protocols where short (< 10 ns) light pulses were applied interleaved by long (seconds) periods in the dark.[10-13] Photoexcitation of the ChR^{470} state leads to a photocycle with four intermediate states: P_1^{500}, P_2^{390}, P_3^{520} and P_4^{480} (see Fig. 1A for a kinetic scheme), the three formers containing 13-*cis* retinal and the latter retinal in all-*trans* configuration.[5] The P_3^{520} intermediate decays monoexponentially with τ = 6-10 ms in detergent-solubilized *Cr*ChR2 (20-25 °C and pH ~ 7)[10,14,15] much as the photocurrents do under equivalent conditions in cells.[15,16] The same good kinetic correlation is preserved in various mutants,[10,16] supporting the conductivity of the P_3^{520} intermediate and the relevance of time-resolved spectroscopic studies of *Cr*ChR2 in detergent.[5] P_4^{480} is a non-conductive intermediate with an unusual slow decay, τ = 5-20 s,[10,17] bypassed by the ~75% of the molecules relaxing back to the ChR^{470} state (Fig. 1A).[10,13]

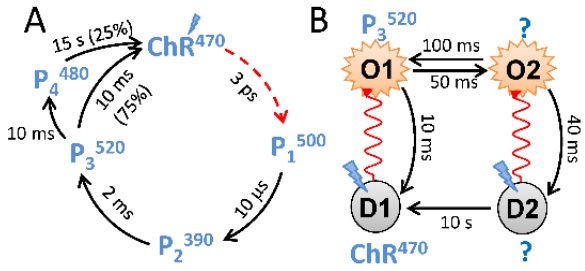

Figure 1. Photocycle models of *Cr*ChR2 with approximate time constants derived from experiments performed under (A) single turnover conditions, with intermediates characterized spectroscopically[5] and (B) multiple turnover conditions, with intermediates conductivities characterized by electrophysiology.[18,19]

In electrophysiological experiments, *Cr*ChR2 is typically excited by trains of light pulses of tens-to-hundreds of milliseconds in length.[2,18] In contrast to laser flash experiments, the photocurrents under these conditions decay bi-exponentially ($\tau_1 \approx$ 4-8 ms and $\tau_2 \approx$ 30-50 ms),[18] and display new phenomena such as inactivation (i.e., stationary photocurrents lower than peak photocurrents) and light adaptation (i.e., decrease of the peak currents with repetitive illumination).[2] A simple model consisting of two intercrossing photocycles, with two non-conductive dark-states (D1 to D2) and two conductive states (O1 and O2), has been employed to quantitatively relate the photocurrents to the intensity, duration, and frequency of the light pulses (Fig. 1B).[18,19] Inactivation emerges from the ~10-to-20-fold lower conductance of O2 with respect to O1 and the increased O2/O1 ratio under sustained illumination,[18,20] while light adaptation originates from the dependence of the D2/D1 ratio on the illumination history.[19]

Desensitization and light adaptation are among the main drawbacks of *Cr*ChR2 as an optogenetic tool.[3] Thus, characterization of the secondary photocycle in *Cr*ChR2 is of immense practical relevance. There is consensus that D1 and O1 correspond to the well-characterized ChR^{470} and P_3^{520} states (Fig. 1B). Instead, the molecular identity of D2 and O2 remains disputed. It has been suggested that D2 corresponds to the ChR^{460} state, the dark state with 13-*cis*,15-*syn* retinal.[8] However, in opposition to this assignment, the decay of ChR^{460} to ChR^{470} takes several hours,[8] while the decay of D2 to D1 proceeds with $\tau \approx 10$ s.[18]

Here, we propose that the D2 state corresponds to the P_4^{480} intermediate, and O2 to one of its photoproducts. To validate this hypothesis, we characterized the photoactivity of P_4^{480} by transient UV/Vis absorption spectroscopy.

RESULTS

The slow decay of the P_4^{480} intermediate, three orders slower than the previous P_3^{520} intermediate,[5] was the basis for our strategy to address the photoreaction of the P_4^{480} state. In contrast to previous time-resolved studies,[10,11] we pre-illuminated the sample using a light emitting diode (LED) to generate a photo-stationary mixture enriched in P_4^{480}.[21] After the LED was switched off, we introduced a variable time delay, Δt, long enough (≥ 1 s) to ensure that all intermediates other than P_4^{480} fully relax to ChR^{470}, an expectation confirmed by time-resolved FTIR experiments (Fig. S1). Subsequently, the sample was excited with a 10 ns laser flash and transient absorption UV/Vis changes were recorded (Fig. 2A top for a scheme).

We measured transient absorption changes at 520 nm with time delays between 1 s to 40 s (Fig. 2A). Additional transients have been recorded at 380 nm and analyzed (Fig. S2). The variable time delays generate different P_4^{480} / ChR^{470} ratios before the sample is interrogated by the laser excitation. For long time delays (e.g., Δt = 40 s), the time trace matches that measured before for the ChR^{470} photocycle, showing contributions from the well-known red-shifted intermediates P_1^{500}, P_3^{520} and P_4^{480} (Fig. 2A).[5] As the time delay is reduced, the time traces at 520 nm gradually change in shape, indicating that: a) P_4^{480} is photoactive and; b) its photocycle contains at least one red-shifted intermediate. A rank analysis by singular value decomposition supports the conclusion that only two photocycles, from ChR^{470} and P_4^{480}, contribute to the time traces in Fig. 2A (see Fig. S3).

The laser flash typically excites less than a 10% of the ChR2 molecules in the ChR^{470} state.[15] A similar incomplete photoexcitiation is anticipated for the P_4^{480} state. As a consequence, the recorded kinetic traces in Fig. 2A also reflect the thermal decay of the unexcited P_4^{480} intermediate back to ChR^{470} (see Fig. S4 for a control experiment without laser flash). This contribution interferes with the recorded time traces above 100 ms (shaded area in Fig. 2A). Being well-described by a single exponential decay its contribution can be numerically corrected when needed (Fig. S5).

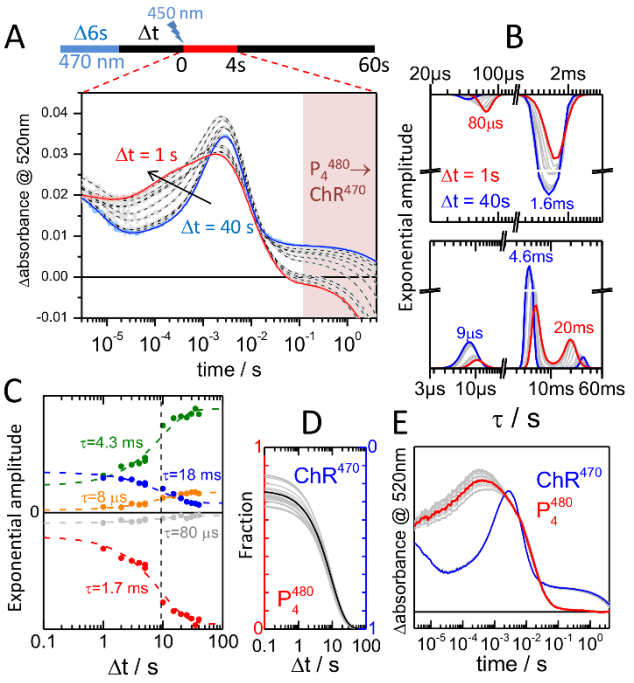

Figure 2. Generation of variable mixtures of ChR^{470} and P_4^{480} states by pre-illumination, and characterization of their transient absorption changes at 520 nm. (A) Kinetic traces at 520 nm (continuous lines), recorded after a variable delay (Δt from 1 s to 40 s) between the end of pre-illumination (470 nm, 6 s, 15 mW/cm^2) and a laser flash (450 nm, 10 ns, 2 mJ/cm^2). Global exponential fitting (dashed lines). The shaded area marks contributions from the P_4^{480}-to-ChR^{470} decay. (B) Lifetime distribution analysis of the time-traces in (A), split in rising (top) and decaying (bottom) components. (C) Exponential amplitudes as a function of Δt (solid circles) globally fitted to a single exponential decay (colored dashed lines) with $\tau = 9.3$ s (vertical dashed line). (D) Estimated population of ChR^{470} and P_4^{480} as a function of Δt (black trace) with uncertainties (grey traces). (E) Estimated pure kinetic traces at 520 nm for the ChR^{470} (blue trace) and P_4^{480} (red trace) photocycles, with uncertainties (grey traces).

We conducted a maximum entropy lifetime distribution analysis of the time traces at 520 nm to discriminate exponential components arising from the ChR^{470} and the P_4^{480} photocycles (Fig. S6). Exponential components are resolved here as bands, which for displaying purposes we split into exponential rising components, giving negative bands (Fig. 2B top), and exponential decaying components, giving positive bands (Fig. 2B bottom). With $\tau \approx 1.6$ ms and $\tau \approx 4.6$ ms we resolve the rise and decay of the P_3^{520} intermediate.[14] As expected, the amplitude of these two components decreases as Δt decreases, (Fig. 2B, compare blue and red curves). On the contrary, two components at $\tau \approx 80$ µs and $\tau \approx 20$ ms, marginally present in the dark-adapted sample, increase their amplitude with shorter values of Δt (Fig. 2B, compare blue and red curves). We assign them to the rise ($\tau \approx 80$ µs) and decay ($\tau \approx 20$ ms) of a red-shifted intermediate in the P_4^{480} photocycle.

Figure 2C shows the exponential amplitudes as a function of Δt, obtained by global exponential fitting of the experimental data (Fig. 2A, dashed traces). All amplitudes exhibit a dependence on Δt well-modeled by a single exponential with $\tau = 9.3 \pm 1.5$ s (Fig. 2C). A similar dependence is observed for the exponential amplitudes of the transients at 380 nm (Fig. S2B).

This recovery time constant agrees with the time constant for the decay of P_4^{480} to ChR^{470} reported in the literature, τ = 6 - 20 s,[10,14,15] confirming that the second photocycle of *Cr*ChR2 observed here originates from photo-excitation of P_4^{480}. Note also the similarity of the data in Fig. 2C with the "peak current vs time delay" plots used in electrophysiology experiments to assess dark adaptation (reversal of light adaptation),[15,22] suggesting a fundamental link between the decay of P_4^{480} to ChR^{470} and the decay of D2 to D1.

The exponential amplitudes in Fig. 2C for the $\tau \approx 1.7$ ms and $\tau \approx 4.3$ ms components take a 24 ± 8% of their maximum value when extrapolated to zero time delay, indicating a mixture of 24 ± 8% ChR^{470} and 76 ± 8% P_4^{480} during continuous illumination. After combining these percentages with the time constant of P_4^{480} decay (9.3 ± 1.5 s, Fig. 2C), we calculated the fractions of P_4^{480} and ChR^{470} as a function of the delay time in the dark (Fig. 2D). And from these fractions we obtained the kinetics at 520 nm for the pure ChR^{470} and P_4^{480} photocycles by least-squares (Fig. 2E).

In order to get further insights into the P_4^{480} photocycle, we recorded a spectral map from 360 nm to 560 nm in 10 nm steps: the sample was pre-illuminated for 6 s with a blue LED, followed by a 3 s delay time in the dark prior to laser flash excitation and data acquisition (Fig. 3A). As a control, we measured a spectral map without pre-illumination (Fig. 3B), corresponding to the ChR^{470} photocycle. We subtracted the data in Fig. 3A and Fig. 3B with a factor of 0.45 (derived from Fig. 2D) to obtain the spectro-temporal changes associated with the P_4^{480} photocycle (Fig. 3C). From the result, we conclude that the photocycle of P_4^{480} contains at least two intermediates: a P_2-like intermediate with $\lambda^{max} \approx 390$ nm (I_2^{390}), and a P_3-like intermediate with $\lambda^{max} \approx 530$ nm (I_3^{530}). Time slices at 520 nm and 380 nm for the ChR^{470} and P_4^{480} photocycles are presented in Figs. 3D and 3E, respectively. Those at 520 nm might contain minor contributions from the 13-*cis* photocycle, but restricted to the microsecond range.[12] The I_2^{390} intermediate rises and decays much earlier than its P_2^{390} homologue, with a very low accumulation (Fig 3E and Fig. S2C). The I_3^{530} intermediate rises earlier and decays slower than its P_3^{520} homologue, showing a similar accumulation level (Fig. 3D-E and Fig. 2E).

We performed a global exponential analysis of the spectral maps in Figs. 3A-C, to obtain eight time constants and their decay associated spectra (DAS) (see Fig. S7). The P_3^{520} intermediate decays with τ = 3.8 ms, as indicated by the positive peak at 520 nm in the corresponding DAS-5 from the ChR^{470} photocycle (Fig. 3F, blue curve). I_3^{530} decays with τ = 17 ms, as supported by the positive peak at 530 nm in DAS-6 from the P_4^{480} photocycle (Fig. 3G, red curve). In addition, the ChR^{470} photocycle shows in DAS-6 a minor but significant positive amplitude at 500 nm (Fig. 3F, blue curve), explaining why the amplitude of the τ = 18 ms component in Fig. 2B,C does not fully decay to zero at long Δt.

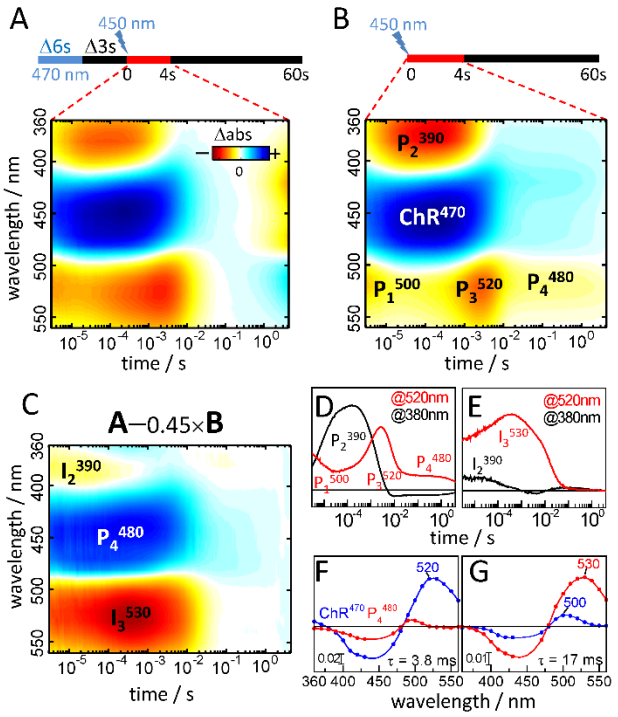

Figure 3. Spectral analysis of the P_4^{480} photocycle. (A) Transient absorption changes of *Cr*ChR2 with pre-illumination and (B) without pre-illumination. (C) Spectral map of the P_4^{480} photocycle, obtained by subtracting data in (A) and (B), and correcting for the P_4^{480}-to-ChR^{470} decay. (D, E) Extracted kinetics at 520 nm and 380 nm for the (D) ChR^{470} and (E) P_4^{480} photocycles. (F, G) Decay associated spectra for (F) τ = 3.8 ms and (G) τ = 17 ms for the ChR^{470} (blue) and P_4^{480} (red) photocycles.

Based on the above results we propose a modified photocycle scheme (Fig. 4), which includes the photoreactions after the sequential absorption of two photons by ChR^{470} and P_4^{480}. The hereby characterized P_4^{480} photocycle shows a P_2-like intermediate, I_2^{390}, which rises with τ < 1 μs. I_2^{390} decays with $\tau \approx 100$ μs to I_3^{530}, a P_3-like intermediate. The I_3^{530} intermediate rises in two phases (see Fig. S8), with τ < 1 μs (65%) and with $\tau \approx 100$ μs (35%), decaying to the parent P_4^{480} state with $\tau \approx 20$ ms.

DISCUSSION

The photocycle of P_4^{480} (Fig. 4) shares two key features with the secondary photocycle of *Cr*ChR2 introduced to model the photocurrents under continuous illumination (Fig. 1B). First, the I_3^{530}-to-P_4^{480} transition is 4-5 times slower than the P_3^{520}-to-ChR^{470} transition ($\tau \approx 4$ ms vs 20 ms), much like the decay of O2-to-D2 is 4-5 times slower than decay of O1-to-D1 ($\tau \approx$ 4-8 ms vs 30-50 ms).[18] Second, P_4^{480} thermally decays to ChR^{470} with $\tau \approx 9.3$ s in wild-type *Cr*ChR2 (Fig. 2C) and with $\tau \approx 3$ s in E123T,[12] much like D2 thermally decays to D1 with $\tau \approx 10$ s in the wild type (Fig. 1B)[18] and with $\tau \approx 1$ s in the E123T variant.[22] Having both ChR^{470} and P_4^{480} an all-*trans* retinal[9] it is conceivable that both photocycles display intermediates with similar properties and, thus, that I_3^{530} is, like P_3^{520}, conductive. Future electrophysiology experiments will be required to confirm the conductivity of the I_3^{530} intermediate, which we expect to be 10-20 times smaller than for the P_3^{520} intermediate

based on the O1/O2 conductivity ratio.[18,20] Overall, the present results are fully consistent with the notion that the P_4^{480} and I_3^{530} intermediates correspond to the non-conductive D2 and conductive O2 states, respectively.

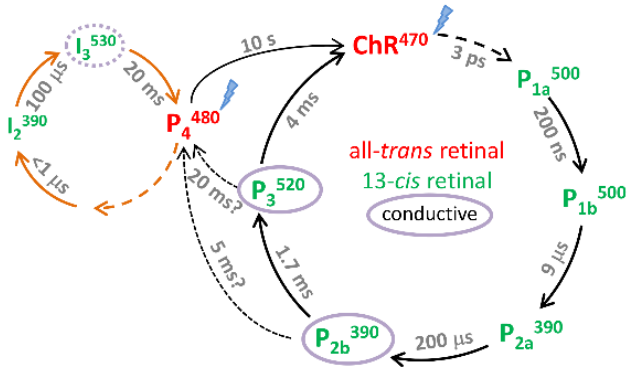

Figure 4. Photocycle model of *Cr*ChR2, including the ChR^{470} photocycle[12,16] and the P_4^{480} photocycle, ignoring possible back-reactions.[23] We assume that I_2^{390} and I_3^{530} hold a 13-*cis* retinal. We hypothesize that the I_3^{530} intermediate is conductive. Time constants for dotted transitions are chosen to allow for 75% of the photo-excited ChR^{470} molecules to bypass the P_4^{480} intermediate.

Our results indicate that the recovery of the photocurrents from light adaptation is controlled by the slow thermal decay of P_4^{480} to ChR^{470}. Why is this decay so slow? Although the P_4^{480} intermediate appears to be structurally similar to P_3^{520},[10,24,25] the decay of P_3^{520} to ChR^{470} is 3 orders of magnitude faster, suggesting that the rate-limiting factor in the decay of P_4^{480} to ChR^{470} is not the reversal of protein conformational changes. The decay of P_4^{480}, but not of P_3^{520}, involves reprotonation of E90.[10] In the E90A variant the decay of P_4^{480} is equally slow though (Fig. S9), indicating that its reprotonation is not rate-limiting either. Both P_4^{480} and ChR^{470} contain all-*trans* retinal, as concluded from retinal C=C vibrations probed by resonance Raman spectroscopy and retinal extraction followed by chromatography.[9] P_4^{480} and ChR^{470} differ in the C–C stretching vibrations of the retinal,[9] indication that the configuration of some C–C bonds might differ between them. Although highly speculative, it is possible that thermal isomerization around C-C bonds of the retinal, for instance from all-*trans*,15-*syn* to all-*trans*,15-*anti*, might be the rate-limiting step in the decay of P_4^{480}.

Given the identity between P_4^{480} and D2, decreasing the formation of the P_4^{480} intermediate should reduce both light adaptation and inactivation of the photocurrents. Thus, understanding the formation of the P_4^{480} intermediate is of utmost relevance to design strategies for this goal. We have proposed that P_4^{480} is formed as a result of a branch in the ChR^{470} photocycle.[5] Because of the structural similarity of P_4^{480} with the P_{2b}^{390} and P_3^{520} intermediates,[10,16,24,25] it is reasonable to assume that the branching takes place at any of these two intermediates, with the competing time constants defining the branching factor and, thus, the accumulation of P_4^{480} (Fig. 4). Another hypothesis are parallel photocycles originated from heterogeneities in ChR^{470},[13] with only a subpopulation of ChR^{470} giving rise to the P_4^{480} intermediate. The recent dimeric X-ray structure of the dark state of *Cr*ChR2 reveals conformational differences between the two protomers for some side chains and internal water molecules,[6] although the relevance of these subtle heterogeneities remains unclear.

The reported photoreactivity of the P_4^{480} intermediate should not come as a complete surprise. It was previously shown that the photoexcitation of the P_2^{390} and P_3^{520} intermediates leads to a fast shutdown of the photocurrents by recovery of the ChR^{470} state.[15,23] In bacteriorhodopsin, photoexcitation of the K, L and M intermediates (13-*cis* retinal) leads also to the recovery of the dark state,[26] while the N intermediate (13-*cis* retinal) displays a more complex photoreaction.[26] Photoexcitation of the O intermediate (all-*trans* retinal) has resulted in contradictory reports,[26] but might involve a photocycle returning back to O through the formation of a N-like intermediate,[27] a process somehow reminiscent to the photocycle of P_4^{480} that we report here.

OUTLOOK

We have established and characterized the photoactivity of the P_4^{480} state of *Cr*ChR2. We have provided evidence for a link between its photocycle and the desensitization of the photocurrents. Further characterization of the P_4^{480} state and its photocycle will provide new perspectives in improving the properties of *Cr*ChR2 as an optogenetic tool.

ASSOCIATED CONTENT

Supporting Information.
Experimental Section and Figures S1-S10. The Experimental Section provides details regarding the preparation of the *Cr*ChR2 sample, the acquisition of time-resolved UV/Vis and FTIR experiments, and their analysis (global exponential fit, lifetime distribution analysis, singular value decomposition, and estimation of pure time-traces for the P_4^{480} photocycle). Figure S1 – Relaxation kinetics of *Cr*ChR2 after pre-illumination monitored by time-resolved rapid-scan FTIR spectroscopy. Figure S2 – Transient absorption changes at 380 nm of pre-illuminated *Cr*ChR2. Figure S3 – Singular value decomposition analysis of the transient absorption changes in Fig. 2A. Figure S4 – Transient absorption changes of pre-illuminated *Cr*ChR2 at 520 nm, without laser excitation. Figure S5 – Correction for the decay of unexcited P_4^{480} to ChR470 in pre-illuminated time-resolved UV/Vis experiments. Figure S6 – Full lifetime distributions from Fig. 2B. Figure S7 – Decay associated spectra from the global fitting of the data in Fig. 3B and 3C. Figure S8 – Lifetime distribution analysis of the kinetics of the P_4^{480} photocycle at 520 nm. Figure S9 – Comparison of the decay kinetics of P_4^{480} in *Cr*ChR2 WT and E90A. Figure S10 – UV/Vis absorption spectrum of the *Cr*ChR2 sample before and after UV/Vis time-resolved experiments.

AUTHOR INFORMATION

Corresponding Author

victor.lorenz@uv.es

ORCID

Victor A. Lorenz-Fonfria: 0000-0002-8859-8347
Ramona Schlesinger: 0000-0002-7716-4439
Joachim Heberle: 0000-0001-6321-2615
Mattia Saita: 0000-0003-0638-1644

Notes

The authors declare no competing financial interests.

ACKNOWLEDGMENT

Funding was provided by the Spanish Ministry of Economy, Industry and Competitiveness though the project BFU2016-768050-P and a Ramon y Cajal fellowship RYC-2013-13114 to V.A.L.-F., and by the German Research Foundation through the SFB-1078, projects B3 to J.H and B4 to R.S.

REFERENCES

(1) Govorunova, E. G.; Sineshchekov, O. A.; Li, H.; Spudich, J. L. *Annu. Rev. Biochem.* **2017**, *86*, 845.

(2) Nagel, G.; Szellas, T.; Huhn, W.; Kateriya, S.; Adeishvili, N.; Berthold, P.; Ollig, D.; Hegemann, P.; Bamberg, E. *Proc. Natl. Acad. Sci U. S. A.* **2003**, *100*, 13940.

(3) Fenno, L.; Yizhar, O.; Deisseroth, K. *Annu. Rev. Neurosci.* **2011**, *34*, 389.

(4) Stehfest, K.; Hegemann, P. *Chemphyschem* **2010**, *11*, 1120.

(5) Lórenz-Fonfría, V. A.; Heberle, J. *Biochim. Biophys. Acta* **2014**, *1837*, 626.

(6) Volkov, O.; Kovalev, K.; Polovinkin, V.; Borshchevskiy, V.; Bamann, C.; Astashkin, R.; Marin, E.; Popov, A.; Balandin, T.; Willbold, D.; Buldt, G.; Bamberg, E.; Gordeliy, V. *Science* **2017**, *358*.

(7) Becker-Baldus, J.; Bamann, C.; Saxena, K.; Gustmann, H.; Brown, L. J.; Brown, R. C.; Reiter, C.; Bamberg, E.; Wachtveitl, J.; Schwalbe, H.; Glaubitz, C. *Proc. Natl. Acad. Sci. U. S. A.* **2015**, *112*, 9896.

(8) Bruun, S.; Stoeppler, D.; Keidel, A.; Kuhlmann, U.; Luck, M.; Diehl, A.; Geiger, M. A.; Woodmansee, D.; Trauner, D.; Hegemann, P.; Oschkinat, H.; Hildebrandt, P.; Stehfest, K. *Biochemistry* **2015**, *54*, 5389.

(9) Nack, M.; Radu, I.; Bamann, C.; Bamberg, E.; Heberle, J. *FEBS Lett.* **2009**, *583*, 3676.

(10) Lórenz-Fonfría, V. A.; Resler, T.; Krause, N.; Nack, M.; Gossing, M.; Fischer von Mollard, G.; Bamann, C.; Bamberg, E.; Schlesinger, R.; Heberle, J. *Proc. Natl. Acad. Sci. U. S. A.* **2013**, *110*, E1273.

(11) Kuhne, J.; Eisenhauer, K.; Ritter, E.; Hegemann, P.; Gerwert, K.; Bartl, F. *Angew. Chem. Int. Ed. Engl.* **2014**, *54*, 4953.

(12) Lórenz-Fonfría, V. A.; Schultz, B. J.; Resler, T.; Schlesinger, R.; Bamann, C.; Bamberg, E.; Heberle, J. *J. Am. Chem. Soc.* **2015**, *137*, 1850.

(13) Szundi, I.; Li, H.; Chen, E.; Bogomolni, R.; Spudich, J. L.; Kliger, D. S. *J. Biol. Chem.* **2015**, *290*, 16573.

(14) Resler, T.; Schultz, B. J.; Lórenz-Fonfría, V. A.; Schlesinger, R.; Heberle, J. *Biophys. J.* **2015**, *109*, 287.

(15) Bamann, C.; Kirsch, T.; Nagel, G.; Bamberg, E. *J. Mol. Biol.* **2008**, *375*, 686.

(16) Lórenz-Fonfría, V. A.; Bamann, C.; Resler, T.; Schlesinger, R.; Bamberg, E.; Heberle, J. *Proc. Natl. Acad. Sci. U. S. A.* **2015**, *112*, E5796.

(17) Verhoefen, M. K.; Bamann, C.; Blocher, R.; Förster, U.; Bamberg, E.; Wachtveitl, J. *Chemphyschem* **2010**, *11*, 3113.

(18) Nikolic, K.; Grossman, N.; Grubb, M. S.; Burrone, J.; Toumazou, C.; Degenaar, P. *Photochem. Photobiol.* **2009**, *85*, 400.

(19) Hegemann, P.; Ehlenbeck, S.; Gradmann, D. *Biophys. J.* **2005**, *89*, 3911.

(20) Richards, R.; Dempski, R. E. *J. Biol. Chem.* **2017**, *292*, 7314.

(21) Ritter, E.; Stehfest, K.; Berndt, A.; Hegemann, P.; Bartl, F. J. *J. Biol. Chem.* **2008**, *283*, 35033.

(22) Gunaydin, L. A.; Yizhar, O.; Berndt, A.; Sohal, V. S.; Deisseroth, K.; Hegemann, P. *Nat. Neurosci.* **2010**, *13*, 387.

(23) Bamann, C.; Gueta, R.; Kleinlogel, S.; Nagel, G.; Bamberg, E. *Biochemistry* **2010**, *49*, 267.

(24) Krause, N.; Engelhard, C.; Heberle, J.; Schlesinger, R.; Bittl, R. *FEBS Lett.* **2013**, *587*, 3309.

(25) Sattig, T.; Rickert, C.; Bamberg, E.; Steinhoff, H. J.; Bamann, C. *Angew. Chem. Int. Ed. Engl.* **2013**, *52*, 9705.

(26) Balashov, S. P. *Isr. J. Chem.* **1995**, *35*, 415.

(27) Tóth-Boconádi, R.; Keszthelyi, L.; Stoeckenius, W. *Biophys. J.* **2003**, *84*, 3857.

SYNOPSIS TOC (Word Style “SN_Synopsis_TOC”). If you are submitting your paper to a journal that requires a synopsis graphic and/or synopsis paragraph, see the Instructions for Authors on the journal’s homepage for a description of what needs to be provided and for the size requirements of the artwork.